

# 120° Hybrid for Bimodal Interferometers

Christian Schweikert, Niklas Hoppe, Wolfgang Vogel, and Manfred Berroth  
 Institute of Electrical and Optical Communications Engineering  
 University of Stuttgart  
 Stuttgart, Germany  
 christian.schweikert@int.uni-stuttgart.de

**Abstract**—An 120° hybrid for bimodal interferometers in the 220 nm silicon-on-insulator technology is presented. Three output signals enable an unambiguous phase detection over a 360°-range as well as a constant sensitivity. The length of the hybrid is only 190 μm with a simulated excess loss of 0.16 dB. Measurements combined with digital signal processing verify the functionality of a fabricated 120° hybrid.

## I. INTRODUCTION

Mach-Zehnder interferometers (MZIs) and bimodal interferometers (BMIs) are established devices for the detection of refractive index changes, e.g. in biosensing. For instance, in [1] a sensor is presented, where a BMI combined with a functional cladding is used to detect the COVID-19 virus. MZIs as well as BMIs can be designed with high temperature stability [2], they have high fabrication tolerances and advanced readout systems can be applied. In lossless balanced excited single-ended systems, the transmission  $T$  can be expressed as

$$T = \frac{1}{2} + \frac{1}{2} \cos(\Delta\phi) \quad (1)$$

with the mutual phase difference  $\Delta\phi$  of the interfering modes. The phase sensitivity  $S$  of the system, defined as the derivation of the transmission over the phase difference, is  $|S| = \frac{1}{2} |\sin(\Delta\phi)|$ . So, in single wavelength operations the sensitivity directly depends on the operation point and the phase can be retrieved unambiguously in a range of 180° only. To overcome these problems a 90° hybrid readout system for the MZI and for the BMI is proposed in [3]. These structures allow the detection of the phase with constant sensitivity and unambiguity over 360°. Also, the device is independent against input power fluctuations like the relative intensity noise from the laser source or unknown modal losses that would directly deteriorate the phase measurement accuracy. In [4] and [5] an MZI is combined with a 3x3 multimode interferometer (MMI) realizing a 120° hybrid. Combined with digital signal processing, same advantages like the 90° hybrid are achievable with smaller footprint. Additionally, the group in [6] compares a 90° with an 120° hybrid in terms of optical receiver for coherent detection. Their investigations show that an 120° hybrid enables an extended dynamic range and a broader operating bandwidth. However, there's no counterpart for BMIs so far. This work presents the design of a compact readout system, that realized such an 120° hybrid.

The optical simulations are based on the eigenmode expansion (EME) in FIMMPROP from Photon Design and they are compared with BeamPROP from RSoft Photonic Device Tools and verified with measurements.

## II. SIMULATION AND MEASUREMENT

Fig. 1(a) illustrates the working principle of the system. The output of the bimodal sensing waveguide enters a mode converter described in [3]. Thereafter, an MMI separates the

transverse-electric fundamental mode (TE0) from the transverse-electric first-order mode (TE1). While the TE0 self-images into the central output port, the TE1 asymmetrically splits into the upper and lower port with a mutual phase shift of 180°. All three signals are in TE0 configuration. A 90° phase shifter follows in the lower arm. A subsequent 3x3 MMI with a length of 69 μm realizes the 120° hybrid. The simulated transmissions are shown in Fig 1(b). Its simulated excess loss (EL) of 0.16 dB is lower than in other reported readout systems [7]. After their detection, the Clarke transformation is applied to convert the three output signals to a complex signal  $\underline{t} = i + jq = |\underline{t}|e^{i(\Delta\phi+\phi_0)}$  with [5]

$$i = O2 - \frac{1}{2}O1 - \frac{1}{2}O3 \quad (2)$$

$$q = \frac{\sqrt{3}}{2} (O1 - O3). \quad (3)$$

The signals  $i$  and  $q$  result as depicted in Fig. 1(c). In the simulated case, the values for different phase shifts plotted in

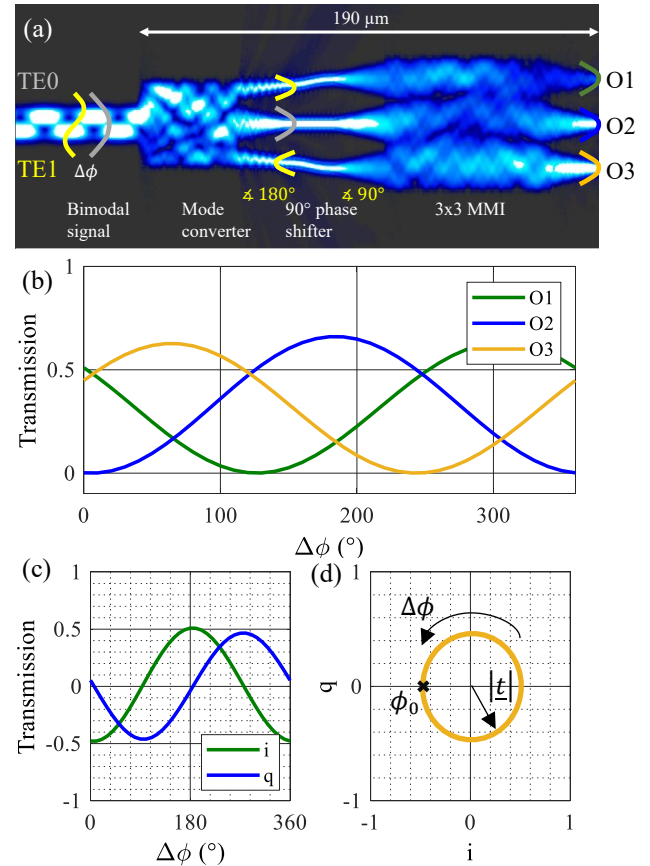


Fig. 1. (a) The architecture of the 120° hybrid with its transmissions in (b) simulated in RSoft. (c) The signals  $i$  and  $q$  after the applied Clarke transformation and (d) plotted in complex plane.

the complex plane are located on a circle with the radius  $|\underline{t}|$ , depicted in Fig. 1(d). The phase offset  $\phi_0$  causes from the  $120^\circ$  hybrid itself and is here  $180^\circ$ . The derivation of  $\underline{t}$  over  $\Delta\phi$  represents the phase sensitivity and results in  $|\underline{t}|$  [5]. In the lossless case,  $|\underline{t}|$  is 1/2 and thus the phase sensitivity corresponds to the maximal achievable value of a single-ended system [5]. However, in the  $120^\circ$  hybrid it is independent of the operation point and thus always constant. In real case, fabrication inaccuracies cause phase and amplitude deviations. To compensate those, the device has to be characterized for a chosen wavelength over a phase difference of  $360^\circ$ , e.g. by performing a measurement series of various refractive index changes. Then advanced digital signal processing can be applied for self-calibration [4].

In this work, the working principle of the readout system and its calibration are validated by the use of the wavelength-dependency of the phase shift. Despite dispersion that affects the measurement, the functionality can be demonstrated. Fig. 2(a) depicts the measured transmissions of a fabricated  $120^\circ$  hybrid over the wavelength. Compared to the proposed  $3 \times 3$  MMI, the length is  $341.2 \mu\text{m}$ . This is a higher-order self-imaging length but has the same functionality as the more compact solution from Fig. 1(a), that has not been produced so far. The depicted bold line is the averaged curve of the thin-plotted measurement without the small ripples. These are undesired artifacts of higher-order modes, resulting from the bimodal excitation in the sensing waveguide. The mode excitation can be optimized to prevent them. For further processing these ripples are calibrated out. After applying the

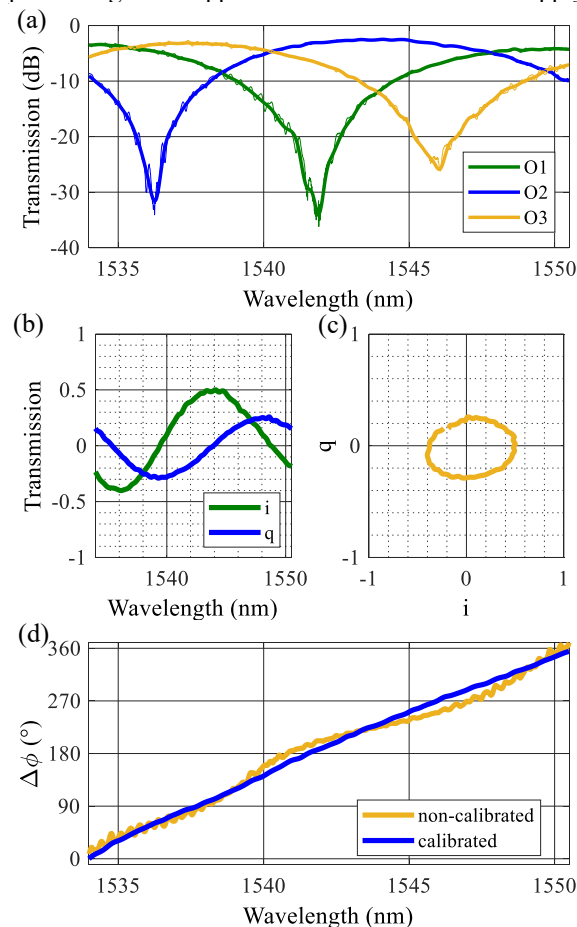


Fig. 2. (a) The measured transmissions of a designed  $120^\circ$  hybrid after a bimodal region. The bold line is the averaged curve without the measured small ripples. (b) The Clarke-transformed signals and (c) depicted in the complex plane. (d) The calculated phase shift with and without calibration.

Clarke transformation, done in software, the curves in Fig. 2(b) result. In the complex plane (see Fig. 2(c)), the signals represent an ellipse. Obviously, there are deviations compared to an ideal circle. To compensate them, following steps are to be applied. First, extract the ellipse center as well as the angle between the major axis and the coordinate system. With this data the ellipse can be moved to the origin of the coordinate system and rotated to match the major axis and the abscissa  $i$ . After scaling the ellipse to a circle, the signal is fully calibrated. In [5] a more precise description of these calibration steps is presented. Fig. 2(d) shows the comparison between a BMI with a non-calibrated as well as a calibrated  $120^\circ$  hybrid readout system. They are referred to  $\Delta\phi = 0^\circ$  as starting point. The phase difference of the calibrated  $120^\circ$  hybrid is clearly improved in terms of linearity and phase resolution.

The measured EL of the system with the  $341.2 \mu\text{m}$ -long  $3 \times 3$  MMI is 0.5 dB at 1535 nm, which is in good agreement with the simulated EL of 0.4 dB.

### III. CONCLUSION AND OUTLOOK

An  $120^\circ$  hybrid for BMIs is presented. With a simulated EL of 0.16 dB and a footprint of  $7.5 \mu\text{m} \times 190 \mu\text{m}$  it is a highly efficient and compact readout system that can be produced with simple fabrication steps. Measurements show the functionality of a fabricated readout system with a footprint of  $7.5 \mu\text{m} \times 470 \mu\text{m}$ . Combined with digital signal processing, including the Clarke transformation and calibration algorithm, the device offers a nearly constant sensitivity, unambiguity over  $360^\circ$  and robustness against input power fluctuations or unknown modal losses. Due to these advantages the system is predestined for single wavelength operation.

### ACKNOWLEDGEMENT

This work is funded by the Deutsche Forschungsgemeinschaft (DFG) under grant no. BE 2256/37-1.

### REFERENCES

- [1] B. Bassols-Cornudella, P. Ramirez-Priego, M. Soler, M. -C. Estévez, H. J. D. Luis-Ravelo, M. Cardena-Rubio, L. M. Lechuga, "Novel Sensing Algorithm for Linear Read-Out of Bimodal Waveguide Interferometric Biosensors," in *Journal of Lightwave Technology*, vol. 40, no. 1, pp. 237-244, 2022.
- [2] N. Hoppe, T. Föhn, P. Diersing, P. Scheck, W. Vogel, M. Félix Rosa, M. Kaschel, M. Bach, and M. Berroth, "Design of an Integrated Dual-Mode Interferometer on 250 nm Silicon-on-Insulator," in *IEEE Journal of Selected Topics in Quantum Electronics*, vol. 23, no. 2, pp. 444-451, 2017.
- [3] C. Schweikert, N. Hoppe, R. Elster, W. Vogel, and M. Berroth, "Improved Phase Detection in On-Chip Refractometers," in *International Conference on Numerical Simulation of Optoelectronic Devices (NUSOD)*, 2021, pp. 113-114.
- [4] D. Kohler, G. Schindler, L. Hahn, J. Milvich, A. Hofmann, K. Länge, W. Freude, and C. Koos, "Biophotonic sensors with integrated  $\text{Si}_3\text{N}_4$ -organic hybrid (SiNOH) lasers for point-of-care diagnostics," in *Light Sci Appl*, vol. 10, no. 1, pp. 64, 2021.
- [5] R. Halir, L. Vivien, X. Le Roux, D. - Xu and P. Cheben, "Direct and Sensitive Phase Readout for Integrated Waveguide Sensors," in *IEEE Photonics Journal*, vol. 5, no. 4, 2013, Art. no. 6800906.
- [6] P. Reyes-Iglesias, I. Molina-Fernández, A. Moscoso-Mártir, and A. Ortega-Moñux, "High-performance monolithically integrated  $120^\circ$  downconverter with relaxed hardware constraints," in *Opt. Express*, vol. 20, no. 5, pp. 5725-5741, 2012.
- [7] N. Hoppe, P. Scheck, R. Sweidan, P. Diersing, L. Rathgeber, W. Vogel, B. Riegger, A. Southan, and M. Berroth, "Silicon Integrated Dual-Mode Interferometer with Differential Outputs," in *Biosensors*; vol. 7, no. 3, pp. 37, 2017.